

EXPLICIT HOMOLOGY REPRESENTATION FOR FINITE GROUPS ACTING ON RIEMANN SURFACES

S. ALLEN BROUGHTON¹  AND LINDEN DISNEY-HOGG^{2,*} 

ABSTRACT. Given a finite group G acting orientably on a surface S of genus $\sigma \geq 2$, the group G acts faithfully on the homology group $H_1(S; \mathbb{Z})$, preserving the symplectic intersection form. The action on S and the homology is determined by a *generating vector*, a tuple of elements of G , generating G and satisfying certain properties. In this note we show how to compute the homology representation, using the generating vector, when S/G has genus 0 and the genus is suitably low. A $2\sigma \times 2\sigma$ representing matrix can be determined for any element in the group, usually for a small set of generators. The matrices are computed with respect to an auto-generated basis for the cellular homology of S , using a regular CW structure on S , derived from the G action. We demonstrate the application of these results by computing *invariant theta characteristics* of the Riemann surfaces S with the algorithm implemented using Sage.

1. INTRODUCTION

1.1. Problem description. If a finite group G acts orientably on a surface S , then G acts on the homology group $H_1(S; \mathbb{Z})$, preserving the symplectic intersection form. If the surface is hyperbolic, i.e., of genus $\sigma \geq 2$, then the action is faithful. For various applications, it is desirable to know this representation explicitly. In this note, we present

¹ DEPARTMENT OF MATHEMATICS, ROSE-HULMAN INSTITUTE OF TECHNOLOGY, TERRE HAUTE, INDIANA, U.S.A.

² DEPARTMENT OF MATHEMATICS, IMPERIAL COLLEGE LONDON, LONDON, U.K.

E-mail addresses: brought@rose-hulman.edu, a.disneyhogg@imperial.ac.uk.

Date: June 2026.

* Corresponding author.

Acknowledgements. LDH is grateful to Josh Fogg for their consultation on the efficiency of sparse matrix methods.

Data Availability. The datasets generated during the current study and the code for their creation/analysis are openly available at https://github.com/DisneyHogg/homology_representation/.

Statements and Declarations. The authors have no relevant financial or non-financial interests to disclose.

an algorithm, implemented in Sage [16] and available from https://github.com/DisneyHogg/homology_representation/, to explicitly determine the representation by using simple geometric information about the quotient surface $T = S/G$, and a generating vector for the action of G (see Section 2.1). Our computational process auto-generates a homology basis $a_1, \dots, a_{2\sigma}$ adapted to the G action. We are then able to specify a $2\sigma \times 2\sigma$ representing matrix for any element of the group, e.g., a small set of group generators. Our algorithm allows for homology coefficients from an arbitrary unital ring; the case of coefficients mod 2 is of special interest.

1.2. Previous work. There are existing methods for computing the homology representation from the data of the generating vector. Initially [10, 11] focused on the relatively simple case when G is cyclic of prime order, later extending to arbitrary G [12], and worked with the fundamental polygon to find a basis of cycles adapted to the automorphism in order to simplify the expression of its action. Finding the adapted homology basis required the application of a rewriting system and repeated Teitze transformations. It was also shown how to compute the intersection form in this adapted basis [13], which required finding a standard representative of each homology class. To our knowledge, no implementation of this algorithm was made publicly available.

An alternative approach was developed in [2], again using the fundamental polygon, now restricting to the case when the quotient surface has genus 0. There, the fundamental polygon for S/G is lifted from the Riemann sphere to tessellate the surface by iteratively acting with the generators of the rotations of the fundamental polygon until the tessellation is complete. This tessellation is then treated as a simplicial complex for which the homology can be computed via standard methodologies. Again intersections of cycles are worked out by finding standard representatives of each homology class and carefully inspecting the order of intersections to determine the sign. Code was provided for this method, available at present from <https://github.com/rojas-ani/sage-routines>, and we use this for comparison.

Neither of these two works discussed the additional problem of determining the action of G on $H_1(S; R)$ when R is a unital ring other than \mathbb{Z} . This may always be worked out from $H_1(S; \mathbb{Z})$ using the universal coefficient theorem, but the method we shall describe here makes clear how to use the ring R from the beginning (providing computational benefit) while also avoiding some of the other difficulties inherent in former methods.

1.3. Applications. Explicit knowledge of the homology representation can be useful for a variety of reasons, including identifying loci in the moduli space of abelian varieties [2, §7], and decomposing Jacobians. In this paper we shall consider the problem of computing the orbits of theta characteristics on S , which requires the homology representation with coefficients taken mod 2 [15, 4]. This makes clear the benefit in having a method for computing the action which works over more general rings than \mathbb{Z} . In §7.4 we shall demonstrate the performance of our algorithm in computing the homology representation mod 2 and see that it outperforms existing methodologies both in terms of runtime and memory usage. As such, we are able to compute the orbits of theta characteristics on curves which were previously unattainable, including certain modular curves.

1.4. Computation. Our computations are done using Sage [16], though Magma [3] or GAP [9] would also work. The motivation for using Sage is its combination of being open-source, written using the clean language of Python, and retaining interfaces to many other mathematical software programs such as GAP, which itself was interfaced with for computation of the permutation action of G on its cosets.

2. PRELIMINARIES

To formulate our problem precisely, we need to sketch the connection between orientable group actions and the homology representation. Throughout the paper, S is a closed Riemann surface of genus σ , G is a finite group that acts upon S and $T = S/G$ is the quotient surface.

2.1. Orientable actions and signatures. The finite group G acts *orientably* on S if there is a monomorphism:

$$(1) \quad \epsilon : G \rightarrow \text{Homeo}^+(S),$$

the group of orientation preserving homeomorphisms of S . If the image consists of conformal automorphisms of S , i.e.,

$$(2) \quad \epsilon : G \rightarrow \text{Aut}(S),$$

we say that G acts *conformally* on S . Every action as in (1) gives rise to a representation on the homology $H_1(S; \mathbb{Z})$.

For every orientable action there is a conformal structure on S , perhaps a multi-parameter family of such structures, preserved by G . These multi-parameter families are made up of so-called equisymmetric strata in moduli space; the strata are connected, smooth quasi-projective varieties [5]. It is well-known that we get the exactly one equivalence class of representations along a stratum [6]. It turns out

that in each genus there are only a finite number of strata, a finite number of groups and a finite number of classes of representations to consider [6].

Two actions ϵ_1, ϵ_2 of G on possibly different surfaces S_1, S_2 are *topologically equivalent* if there is an intertwining homeomorphism $h : S_1 \rightarrow S_2$ and an automorphism $\omega \in \text{Aut}(G)$ such that:

$$(3) \quad \epsilon_2(g) = h\epsilon_1(\omega(g))h^{-1}, \quad \forall g \in G,$$

or in diagram form:

$$(4) \quad \begin{array}{ccc} G & \xrightarrow{\epsilon_2} & \text{Homeo}^+(S_2) \\ \downarrow \omega & & \downarrow Ad_h^{-1} \\ G & \xrightarrow{\epsilon_1} & \text{Homeo}^+(S_1) \end{array}$$

where $Ad_x(y) = xyx^{-1}$ whenever the composition is well defined. If h is a conformal map then we say that the actions are conformally equivalent.

The quotient surface $T = S/G$ of an orientable action is a closed, orientable Riemann surface of genus τ , and the quotient map

$$(5) \quad \pi_G : S \rightarrow T$$

is branched over t *branch points* $\{z_1, \dots, z_t\} := B_G \subset T$. At each point \tilde{z}_j lying over z_j , the stabilizer $G_{\tilde{z}_j}$ is a cyclic group of order n_j . We call $\mathfrak{s} = (\tau; n_1, \dots, n_t)$ the *signature* of the action. The relation between the genus, the group order, and the signature is given by the Riemann-Hurwitz equation

$$(6) \quad \frac{2\sigma - 2}{|G|} = 2\tau - 2 + t - \sum_{j=1}^t \frac{1}{n_j}.$$

2.2. The homology representation. Given a group action ϵ , we define the homology representation

$$\rho : G \rightarrow Sp_{2\sigma}(\mathbb{Z})$$

by setting $\rho(g) = \epsilon(g)_*$ to be the automorphism of $H_1(S; \mathbb{Z})$ induced by the homeomorphism $\epsilon(g)$ of S . Since G preserves the non-degenerate intersection form on $H_1(S; \mathbb{Z})$, and $H_1(S; \mathbb{Z})$ is a free \mathbb{Z} -module the representation has its image in the integral symplectic group $Sp_{2\sigma}(\mathbb{Z})$. In a suitable basis the matrices have the form

$$\rho(g) = \begin{bmatrix} A & B \\ -B & A \end{bmatrix}$$

for matrices $A, B \in SL_\sigma(\mathbb{Z})$. If two actions ϵ_1, ϵ_2 of G are equivalent as in equation (3) then the homology representations ρ_1, ρ_2 are equivalent in the sense that

$$(7) \quad \rho_2(g) = U\rho_1(\omega(g))U^{-1}, \quad \forall g \in G,$$

where the matrix U is the induced map $h_* : H_1(S_1; \mathbb{Z}) \rightarrow H_1(S_2; \mathbb{Z})$ with respect to the corresponding bases.

Remark 1. *Note that if $\omega = Ad_g$ is an inner automorphism then it can be absorbed into the matrix U i.e., $U' = U\rho_1(g)$. Therefore, the equivalence class of a representation is not affected by inner automorphisms. Since topological equivalence involves the entire automorphism group of G we do have to consider the $\text{Out}(G)$ action upon the representations.*

Remark 2. *Of course, G acts upon the homology $H_1(S; R)$ and cohomology $H^1(S; R)$ when R is any unital ring. The case of most importance to application is mod 2 coefficients where $R = \mathbb{Z}_2$, see Remark 13 and §7.4.*

2.3. Fundamental groups and generating vectors.

Actions and monodromies. It is typical practice to use Fuchsian group pairs $\Pi \triangleleft \Gamma$ and surface kernel epimorphisms

$$(8) \quad \Pi \hookrightarrow \Gamma \xrightarrow{\eta} G$$

to analyze G -actions. However, since we are considering actions in the topological category, we will utilize an equivalent method using fundamental groups and covering spaces for our constructions.

Set $T^\circ = T - B_G$ and let $S^\circ = \pi_G^{-1}(T^\circ)$. Then the restricted map

$$(9) \quad \pi_G : S^\circ \rightarrow T^\circ$$

is a regular, unramified covering space whose group of deck transformations

$$\text{Gal}(\pi_G) = \text{Gal}(S^\circ/T^\circ) = \{\phi \in \text{Aut}(S^\circ) : \pi_G \circ \phi = \pi_G\}$$

equals $\epsilon(G)$, restricted to S° . This covering determines a normal subgroup $\Pi_G = \pi_1(S^\circ) \triangleleft \pi_1(T^\circ)$ and an exact sequence

$$\Pi_G \hookrightarrow \pi_1(T^\circ) \xrightarrow{\lambda} \text{Gal}(S^\circ/T^\circ) = \epsilon(G)$$

by lifting loops to deck transformations. Combine the map λ with $\epsilon(G) \xrightarrow{\epsilon^{-1}} G$ to get an exact sequence

$$(10) \quad \Pi_G \hookrightarrow \pi_1(T^\circ) \xrightarrow{\xi} G.$$

Any surjective map $\xi : \pi_1(T^\circ) \rightarrow G$ is called a *monodromy*. Monodromies and generating vectors, discussed below, will be our basic starting point for specifying actions.

Since we have left out base points to simplify the exposition, λ and ξ are ambiguous up to inner automorphisms. However, this is no concern according to Remark 1, since we only looking at homology actions up to inner automorphisms. The relation among ϵ , λ and ξ is

$$(11) \quad \xi = \epsilon^{-1} \circ \lambda \text{ or } \epsilon = \lambda \circ \xi^{-1}.$$

The right hand side of the equation makes sense as any two ξ -preimages γ, γ' of $g \in G$ satisfy $\gamma' = \gamma\delta$ with $\delta \in \Pi_G$, and the elements of $\Pi_G = \pi_1(S^\circ)$ have only trivial lifts. For a brief discussion on base points and path lifting, see Section 2.4.

In the opposite direction, suppose we start with an exact sequence as in equation (10). Selecting a conformal structure on T and using the exact sequence, we can construct an unramified, holomorphic, regular covering space which we still denote $\pi_G : S^\circ \rightarrow T^\circ$. The deck transformations in $\text{Gal}(\pi_G)$, found by path lifting, are automatically holomorphic. We define $\epsilon : G \rightarrow \text{Aut}(S^\circ)$ by the second equation in (11). We can fill in the punctures to get a closed surface and the restricted action ϵ extends to a conformal action $\epsilon : G \rightarrow \text{Aut}(S)$ at the filled in punctures using the Removable Singularity Theorem.

Generating vectors. The fundamental group $\pi_1(T^\circ)$ has the following presentation:

$$(12) \quad \text{generators} : \{\alpha_i, \beta_i, \gamma_j \mid 1 \leq i \leq \tau, 1 \leq j \leq t\},$$

$$(13) \quad \text{relations} : \prod_{i=1}^{\tau} [\alpha_i, \beta_i] \prod_{j=1}^t \gamma_j = 1.$$

Define

$$a_i = \xi(\alpha_i), b_i = \xi(\beta_i), c_j = \xi(\gamma_j),$$

then the $2\tau + t$ tuple $(a_1, \dots, a_\tau, b_1, \dots, b_\tau, c_1, \dots, c_t)$ is called a *generating vector* for the action. We observe that

$$(14) \quad G = \langle a_1, \dots, a_\tau, b_1, \dots, b_\tau, c_1, \dots, c_t \rangle,$$

$$(15) \quad o(c_j) = n_j, \text{ and}$$

$$(16) \quad \prod_{i=1}^{\tau} [a_i, b_i] \prod_{j=1}^t c_j = c_1^{n_1} = \dots = c_t^{n_t} = 1$$

for some integers $n_j \geq 2$. We call $(\tau; n_1, \dots, n_t)$ the signature of the action. This definition agrees with that given at the end of Section 2.1.

Proposition 3. *Once an ordered generating set for $\pi_1(T^\circ)$, as in (12), has been fixed, there is a 1-1 correspondence between monodromies and generating vectors.*

2.4. Path lifting and dependence on base points. We make a few remarks on path lifting and base points as they will be needed for the computation of equivariant cellular homology in Section 4. Given ϵ , the maps λ and ξ are dependent on a choice of a base point $w_0 \in T^\circ$ and lift point \widetilde{w}_0 lying over w_0 . Specifically, for $\gamma \in \pi_1(T^\circ, w_0)$, we define the fibre action on the $\pi_G^{-1}(w_0)$ by:

$$(17) \quad \lambda(\gamma) \cdot \widetilde{w}_0 = \widetilde{\gamma}(1),$$

where $\widetilde{\gamma} : [0, 1] \rightarrow S^\circ$ is the π_G -lift of γ satisfying $\widetilde{\gamma}(0) = \widetilde{w}_0$. Since the cover (9) is regular $\lambda(\gamma)$ is actually a deck transformation in $\text{Gal}(\pi_G) = \epsilon(G)$. It can be shown that if another lift point \widetilde{w}_0' is selected then the new lifting action λ' satisfies $\lambda'(\gamma) = \epsilon(x)\lambda(\gamma)\epsilon(x)^{-1}$ for any $\gamma \in \pi_1(T^\circ, w_0)$ and some $x \in G$. In fact we may choose x to satisfy $\epsilon(x) = \lambda(\gamma')$ where the loop γ' is chosen so that $\widetilde{\gamma}'$ is a path from \widetilde{w}_0' to \widetilde{w}_0 . It follows from equation (11) that the choice of a lift point affects the monodromy ξ only by an inner automorphism. If the monodromy ξ is given first, then the action ϵ is modified by an inner automorphism of $\text{Gal}(\pi_G)$.

Now consider the effect of varying the base point w_0 . Let $w_1 \in T^\circ$ be some other base point and δ a path in T° from w_0 to w_1 . Then $\text{Ad}_\delta : \gamma \rightarrow \delta * \gamma * \delta^{-1}$ is an isomorphism

$$\text{Ad}_\delta : \pi_1(T^\circ, w_1) \rightarrow \pi_1(T^\circ, w_0).$$

The lifting homomorphisms λ_0, λ_1 , based at $\widetilde{w}_0, \widetilde{w}_1$, respectively, fit with the map Ad_δ into the diagram:

$$(18) \quad \begin{array}{ccc} \pi_1(T^\circ, w_1) & \xrightarrow{\lambda_1} & \text{Gal}(S^\circ/T^\circ) \\ \downarrow \text{Ad}_\delta & & \downarrow \text{Ad}_\phi \\ \pi_1(T^\circ, w_0) & \xrightarrow{\lambda_0} & \text{Gal}(S^\circ/T^\circ) \end{array}$$

i.e., for some $\phi \in \text{Gal}(S^\circ/T^\circ)$

$$(19) \quad \lambda_0(\delta * \gamma * \delta^{-1}) = \phi \lambda_1(\gamma) \phi^{-1}.$$

To see this, first consider the case where $\widetilde{\delta}$ is a path from \widetilde{w}_0 to \widetilde{w}_1 . The lift $\delta * \widetilde{\gamma} * \delta^{-1}$ has three stages:

- $\widetilde{\delta}$ from \widetilde{w}_0 to \widetilde{w}_1 ,
- $\widetilde{\gamma}$ from \widetilde{w}_1 to $\lambda_1(\gamma) \cdot \widetilde{w}_1$, and
- $(\widetilde{\delta}^{-1})'$ from $\lambda_1(\gamma) \cdot \widetilde{w}_1$ to $\lambda_0(\delta * \gamma * \delta^{-1}) \cdot \widetilde{w}_0$,

where we use a prime to indicate that the lift does not start at the standard starting point. The two paths $\lambda_1(\gamma) \cdot \widetilde{\delta}^{-1}$ and $(\widetilde{\delta}^{-1})'$ both project to δ^{-1} and have the same starting point. So, by unique path lifting and since $\text{Gal}(S^\circ/T^\circ)$ acts without fixed points, then

$$\lambda_0(\delta * \gamma * \delta^{-1}) = \lambda_1(\gamma).$$

So, in this case, equation (19) holds with $\phi = \text{Id}$.

Now suppose that δ is a path from \widetilde{w}_0 to $\widetilde{w}_1' \neq \widetilde{w}_1$. Construct a path $\delta' \in \pi_1(T^\circ, w_1)$ with a lift $\widetilde{\delta}'$ from \widetilde{w}_1' to \widetilde{w}_1 . By the previous case

$$\lambda_0((\delta * \delta') * \gamma' * (\delta * \delta')^{-1}) = \lambda_1(\gamma'),$$

for any $\gamma' \in \pi_1(T^\circ, w_1)$. Pick $\gamma' = (\delta')^{-1} * \gamma * \delta'$ and we get

$$\lambda_0(\delta * \gamma * \delta^{-1}) = \lambda_1((\delta')^{-1} * \gamma * \delta') = \lambda_1(\delta')^{-1} \lambda_1(\gamma) \lambda_1(\delta').$$

We pick $\phi = \lambda_1(\delta')^{-1}$ to get equation (19).

3. EQUIVARIANT CELL-COMPLEX HOMOLOGY ON S

Having explained the theory of how a generating vector determines monodromy, we shall explain how we can use this to compute the homology of S and the action of G upon it in the framework of CW -complexes and cellular homology. For a reference on CW -complexes, computing cellular homology, and the cellular boundary formula see [14]. The discussion shall follow the development in [7].

3.1. Setting up the equivariant tiling on S .

Lifting maps on surfaces. We can create a G -equivariant cell complex on S , suitable for computing homology, by lifting a *map*, i.e. a 2-dimensional cell complex, from T to S . To this end, let \mathcal{E} be a connected, undirected graph, embedded in T , such that the following hold.

- (1) The *vertex set* of \mathcal{E} contains all the branch points, B_G , and possibly some regular points.
- (2) The *edges* of \mathcal{E} are smooth loops or undirected arcs that meet at vertices only and the tangent directions at a vertex are all distinct.
- (3) The complement $T - \mathcal{E}$ is a disjoint union of open topological disks called *faces*, using graph theoretic terminology. We think of the faces as open polygons whose “ideal boundary” consists of edges, concatenated to form a topological circle. The actual boundary may be quite different.

An example of such a graph is given in the left panel of Figure 1, where it is called a *cut-system*. The complement has a single face. A model of the corresponding open polygon (and its homeomorphic lift to S) is

shown in the right panel, along with its ideal boundary. The ramified nodes are numbered and coloured black. The regular nodes are white. The labelling of the polygon vertices will be explained in Section 4.2.

Remark 4. *For our purposes, any surface-graph pair (U, \mathcal{G}) is a map, provided that the following conditions are met. The surface U is closed and orientable and the graph \mathcal{G} is a connected, undirected graph, embedded in U satisfying items 2 and 3 above. We do not consider the case where U is not orientable.*

Notation 5. *The lift to S of a vertex, edge, face, or subgraph of \mathcal{E} may be denoted by decorating the object with a tilde, as previously done in §2. For example, $\tilde{\mathcal{E}}$ is the lift of \mathcal{E} to S and $(S, \tilde{\mathcal{E}})$ is the lift of the map (T, \mathcal{E}) . To keep notation simple, we only use the tilde decoration to eliminate confusion, as in the examples $\tilde{\mathcal{E}}$ and $(S, \tilde{\mathcal{E}})$.*

The lift $\tilde{\mathcal{E}}$ of \mathcal{E} to S defines a map on S . For, the cover π_G introduced in equation (9) is unramified away from B_G and the inverse image of an open face in $T - \mathcal{E}$ is a disjoint union of $|G|$ homeomorphic lifts of the given face to $S - \tilde{\mathcal{E}}$. Likewise, each open edge in \mathcal{E} lifts to $|G|$ open edges in $\tilde{\mathcal{E}}$. Because the cover π_G is regular with deck transformation group $\epsilon(G)$, G acts freely on the sets of open faces and open edges of S .

In [7], the case of lifting a single-faced map (T, \mathcal{E}) to $(S, \tilde{\mathcal{E}})$ was studied in detail. The graph \mathcal{E} was called a *cut system* and the components of the lifted open face were called *polygons* (again see Figure 1). Criteria for determining when the lifted map $(S, \tilde{\mathcal{E}})$ was a regular *CW*-complex (see Section 3.2) were specified. In the regular *CW* case, for each open edge $e \in \mathcal{E}$, exactly two of the edges in the total lift $\pi_G^{-1}(e)$ are included in the boundary of a lifted polygon \mathcal{P} . Finally, if T is topologically a sphere, then the cut system \mathcal{E} is a tree.

3.2. CW-complexes. Let us set up our notation for the structure of a *CW* complex X so that we may use it in the calculation of cellular homology. A general *CW*-complex X is given by the disjoint union:

$$X = \bigcup_n \bigcup_{i \in I_n} C_i^n,$$

where C_i^n is an open cell of dimension n , homeomorphic to the interior of B_i^n , a copy of the closed unit ball in \mathbb{R}^n . There is a separate index set I_n for each dimension n . The n -skeleton is the union of cells of dimension n or lower:

$$X^n = \bigcup_{m \leq n} \bigcup_{i \in I_m} C_i^m.$$

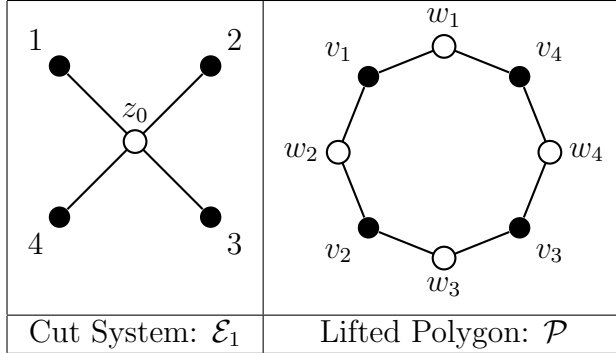


FIGURE 1. Cut system and polygon

We denote the attaching map of C_i^n by

$$\alpha_i^n : \partial B_i^n \rightarrow X^{n-1}.$$

In a *regular CW-complex* X , we require that the closure in X of each open n -dimensional cell C_i^n be homeomorphic to the closed unit ball in \mathbb{R}^n , i.e., the embedding $C_i^n \rightarrow X^n$ extends to an embedding of the closed ball $B_i^n \rightarrow X^n$. Though regularity is not needed for computing cellular homology and the G action on homology, for our purposes it is convenient and no cost to assume regularity for computing boundary maps in cellular chain complexes.

For the complex X determined by the map (U, \mathcal{G}) , $X^0 = \text{vertex set}$, $X^1 = \mathcal{G}$, $X^2 = U$ and all higher skeletons equal U . Regularity is easy to determine for a map (U, \mathcal{G}) , given by the following condition.

- (1) Dimension 1: The closure of each 1-cell in \mathcal{G} is an undirected arc or loop with no internal self intersections. For regularity, there can be no loops.
- (2) Dimension 2: For each closed face f in U , the boundary, ∂f , is a closed subgraph of \mathcal{G} . For regularity, the boundary must be a closed cycle in \mathcal{G} , there can be no self intersections.

Remark 6. *If (T, \mathcal{E}) is regular as a CW complex then the lift $(S, \tilde{\mathcal{E}})$ is also regular as a CW complex.*

3.3. Computing cellular homology. We develop our process for computing equivariant homology for any map on a surface, though when we get to computing specific examples, we will consider only planar actions (where T has genus 0) and will choose lifts of specific maps on the sphere with one or two faces. This will simplify computation and directly relate the computation to the generating vector.

There is a standard way to compute the homology groups of a *CW*-complex, X , which we will apply to the case of a map (U, \mathcal{G}) . We may use the *cellular chain complex*

$$(20) \quad \cdots H_{n+1}(X^{n+1}, X^n) \xrightarrow{\partial_{n+1}} H_n(X^n, X^{n-1}) \xrightarrow{\partial_n} H_{n-1}(X^{n-1}, X^{n-2}) \cdots$$

to compute homology, via the isomorphism

$$(21) \quad H_n(X) \simeq \ker(\partial_n) / \text{im}(\partial_{n+1}).$$

Of course, we need to identify $H_n(X^n, X^{n-1})$ and the differentials ∂_n . By using the homology excision theorem, we have:

$$(22) \quad H_n(X^n, X^{n-1}) \simeq \bigoplus_{i \in I_n} H_n(B_i^n, \partial B_i^n) = \bigoplus_{i \in I_n} \mathbb{Z}\beta_i^n,$$

where β_i^n represents a positively oriented generator of $H_n(B_i^n, \partial B_i^n)$. If we impose a geometric orientation on the n cells the β_i^n will be determined.

Alternatively,

$$(23) \quad H_n(X^n, X^{n-1}) = \tilde{H}_n(X^n/X^{n-1}),$$

where \tilde{H} is reduced homology and X^n/X^{n-1} is the identification space obtained by collapsing the subspace X^{n-1} to a point. The space X^n/X^{n-1} is homeomorphic to a wedge of n -spheres, one for each C_i^n .

Notation 7. *Typically, for the geometric realization of an n -cell we shall use terminology and the associated notation of maps on surfaces, especially when considering a specific case. So, we use the terms and notation for branch point, vertex, edge, face, and polygon. On the other hand, especially when discussing the general, regular case, it may be simpler to let β_i^n stand for the geometric realization of an n -cell with boundary. Likewise, in a specific case, we may use the geometrical objects noted above when discussing cellular boundary maps.*

Next, we need to define ∂_n and state the cellular boundary formula (25). The differential ∂_n is the composition of standard boundary and inclusion maps in homology:

$$(24) \quad \partial_n : H_n(X^n, X^{n-1}) \xrightarrow{\partial} H_{n-1}(X^{n-1}) \xrightarrow{j} H_{n-1}(X^{n-1}, X^{n-2}).$$

Then, *the cellular boundary formula* (see [14]) is:

$$(25) \quad \partial_n(\beta_i^n) = \sum_{j \in I_{n-1}} d_{i,j} \beta_j^{n-1},$$

where $d_{i,j}$ is the degree of a map to be described next.

The cell B_i^n is attached to the $n - 1$ skeleton by an attaching map

$$\alpha_i^{n-1} : \partial B_i^n = S_i^{n-1} \rightarrow X^{n-1}.$$

We follow this by a quotient map

$$q_j^{n-1} : X^{n-1} \rightarrow S_j^{n-1}$$

obtained by collapsing all the spheres in X^n/X^{n-1} to a point except the one corresponding to C_j^{n-1} . Then $q_j^{n-1} \circ \alpha_i^{n-1}$ is a self-map of the $n - 1$ sphere, so we may define

$$(26) \quad d_{i,j} = \text{degree}(q_j^{n-1} \circ \alpha_i^{n-1}).$$

Remark 8. *The formula (25) shows that ∂_n is represented by the integer matrix $[d_{i,j}]$. For a regular cell complex the combined map $q_j^{n-1} \circ \alpha_i^{n-1}$ is a homeomorphism, resulting in $d_{i,j} = \pm 1$, by (26).*

4. HOMOLOGY OF MAPS ON A SURFACE

4.1. Computational considerations and assumptions. We will now impose regularity upon our surface map (U, \mathcal{G}) . We need to give each 2-cell and 1-cell an orientation, these orientations will determine the choices for β_i^2 and β_j^1 . The orientation on the surface defines an orientation on each 2-cell, in turn telling us the sequence of edges and their directions in a counterclockwise circuit around the cell boundary. The orientations of the 1-cells may need to be picked arbitrarily since we can have two different induced orientations from the 2-cells that contain the edge in their common boundary. By regularity, $q_j^1 \circ \alpha_i^1$ is a self-homeomorphism, and $d_{i,j} = 1$ if the counter-clockwise circuit about the boundary of the face labelled i travels along the edge labelled j in the assigned direction. If the direction is opposite then $d_{i,j} = -1$.

Since our calculation of homology is going to involve linear algebra computations using the matrices described in Remark 8, we should try to make these matrices as small as possible so that the construction of the matrices from the generating vector is as easy as possible. As such we construct the map (T, \mathcal{E}) with the following conditions in mind.

- (1) The lifted map is a regular CW -complex.
- (2) The number of lifted 2-cells, 1-cells, and 0-cells are as small as practical.
 - The number of 2-cells is $|G| \times |F|$, where $|F|$ is the number of faces of (T, \mathcal{E}) .
 - The number of 1-cells is $|G| \times |E|$, where $|E|$ is the number of edges of (T, \mathcal{E}) .

- The number of 0-cells is

$$|G| \times \left(|W| + \sum_{j=1}^t \frac{1}{n_j} \right),$$

where $|W|$ is the number of regular nodes in (T, \mathcal{E}) .

- (3) The labelling and orientation of the cells, and hence the determination of $d_{i,j}$, can be done efficiently, just using a generating vector. This allows for efficient coding in Sage.

Remark 9. *We will consider two different cases for the map (T, \mathcal{E}) , one with a single face, $(\mathcal{E} = \mathcal{E}_1)$ and the second with two faces $(\mathcal{E} = \mathcal{E}_2)$. The single faced case generalizes in a nice way when the genus of T is greater than 1. The two faced case is a better for vizualization (black and white tiles) and computation, even though the intermediate matrices are somewhat bigger.*

We are going to make some assumptions on our vertices, edges, and faces of the quotient (T, \mathcal{E}) and the equivariant tiling $(S, \tilde{\mathcal{E}})$, in order to efficiently compute the cellular homology. The validity of the assumptions depends on choices made for \mathcal{E} , a preferred face f on T , a basepoint w in the interior of f , and a generating set for $\pi_1(T^\circ, w)$. Despite having made all these choices, we will capture all homology representations up to standard representation equivalence and the action of $\text{Out}(G)$ on homology representations.

Assumption 10. *As noted previously, G acts freely on the open 1-cells and 2-cells. Considering β_k^1 and β_l^2 as geometric cells with boundary, we may enumerate the cells as pairs (g, β_k^1) and (g, β_l^2) where β_k^1 and β_l^2 range over a set of distinguished orbit representatives of the 1-cells and 2-cells. The boundary maps ∂_n are dependent on the representatives so we are going to make these assumptions.*

- (1) *All the edges and vertices of \mathcal{E} occur on the boundary of every face in $T - \mathcal{E}$.*
- (2) *Let β^2 be a fixed but arbitrary face of S . Then for each 1-cell β^1 (edge) and 0-cell β^0 (vertex), the orbits $G \cdot \beta^1$ and $G \cdot \beta^0$ have representatives that lie in the geometric boundary $\partial\beta^2$ of the face β^2 .*
- (3) *For each face in f in $T - \mathcal{E}$, each branch point z_j occurs exactly once in the idealized boundary of f . We may chose a preferred face f in $T - \mathcal{E}$ such that branch points are in the cyclic order z_1, \dots, z_t , when we travel counter-clockwise along the idealized boundary ∂f .*

- (4) For every face β^2 of S , a ramified vertex v_j , lying over z_j , occurs exactly once in $\partial\beta^2$. Moreover, for those faces β^2 lying over the preferred face f , the vertices are in the cyclic order v_1, \dots, v_t , when we travel counter-clockwise along $\partial\beta^2$.
- (5) Let (c_1, \dots, c_t) be the generating vector of the action. Then there is a distinguished face β_0^2 such that the ramified vertices $v_j \in \partial\beta_0^2$ have the following stabilizers:

$$\text{Stab}_G(v_j) = \langle c_j \rangle,$$

and the local action of c_j at v_j is a counter-clockwise rotation through $2\pi/n_j$ radians.

Our assumptions may seem a little ambitious, but they are not. The construction of \mathcal{E}_1 and \mathcal{E}_2 in Sections 4.2 and 4.3 were specialized so that items 1 and 3 would hold.

Item 2 follows directly from item 1. To prove item 4, note that the open faces of S lift homeomorphically from the open faces of $T - \mathcal{E}$. In addition, the orientation on S , and hence upon its 2-faces may be assumed to be lifted from T since π_G is a holomorphic map.

To prove item 5 we first select w in the interior of our preferred face f on T . We may choose a generating set for $\pi_1(T^\circ, w)$ such that the generator γ_j encircles z_j exactly once in the counter-clockwise direction. These generators are described in some detail in Section 4.3. We compute all generating vectors for the various monodromies ξ with respect to this basis (see Proposition 3). Now pick any distinguished face β_0^2 and $\tilde{w} \in \beta_0^2$ lying over w . The lifting map λ and hence ϵ is computed with respect to this lifted base point. From the discussion in Section 2.4 on lifting and base points, we see that action of $c_j = \xi(\gamma_j)$ is given by the lift $\lambda(\gamma_j)$ based at \tilde{w} . The local character of this lift may be directly examined to prove item 5.

4.2. The single faced case.

Labelling lifted cells in the single faced case. Now we turn specifically to the map $(S, \tilde{\mathcal{E}})$, for the cut system $\mathcal{E} = \mathcal{E}_1$ and a lifted polygon \mathcal{P} illustrated in Figure 1. The black nodes correspond to the branch points z_j with the same numbering. The white node $z_0 \in \mathcal{E}$ is a regular point introduced to make the lifted map CW -regular. The diagram for a different number $t \geq 3$ of branch points is similar, with the proper branch points z_j , $1 \leq j \leq t$, arranged on a circle centred at z_0 and j cyclically increasing in clockwise order. The edges of \mathcal{E} are the *spokes* $e_j = (z_0, z_j)$, emanating from z_0 along a radial line to the branch point z_j . Notice that in a general cut-system with a CW -regular lift, the

number of lifts of a vertex lying on $\partial\mathcal{P}$ equals the valence of that vertex in \mathcal{E} . So, in the case at hand, each proper branch point z_j lifts to a unique vertex on $\partial\mathcal{P}$, denoted v_j , and the white node z_0 lifts to t distinct white nodes w_j , $1 \leq j \leq t$. See Figure 1 for an illustration of the lifted vertices v_j and w_j .

We follow the method and notation of [7] to determine the counter-clockwise labelling of the sequence of lifted edges and nodes on $\partial\mathcal{P}$. We construct a ribbon graph \mathcal{R} , which is a disc neighbourhood of \mathcal{E} , as illustrated in Figure 2. The boundary $\partial\mathcal{R}$, suitably oriented, will determine the labelling and orientation of the vertices and edges in $\partial\mathcal{P}$. First, include in \mathcal{R} a small red disc about each branch point and the white node, so that the system of discs is disjoint, and such that each red disc only meets the spokes incident with the node at the centre of the red disc. Next, for each spoke construct two line segments parallel and very close to the spoke, on each side of the spoke. Include in \mathcal{R} the area between each pair of parallel segments including the spoke. These are the green ribbons in Figure 2.

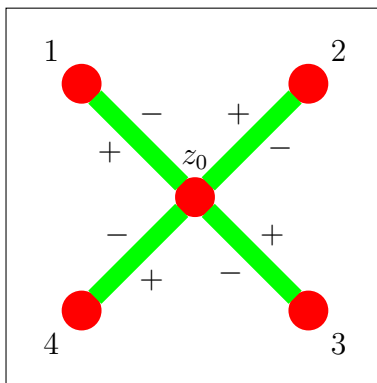


FIGURE 2. Ribbon graph for \mathcal{E}_1 , with orientation markings

A clockwise circuit along $\partial\mathcal{R}$ is a counter-clockwise circuit in the open face $T - \mathcal{E}_1$, very close to its boundary. The circuit is a concatenation of paths doing the following:

- start near z_0 and travel outward along a parallel close to the edge e_j ,
- make a tight clockwise turn about the branch point z_j , along the boundary of the red disc,
- return to z_0 along the opposite parallel of e_j .

In Figure 2 the direction of travel along the edges of the green ribbons in \mathcal{R} is indicated by a $+$ sign (outward travel), or $-$ sign (inward

travel). The lift \widetilde{R} of the ribbon graph meets the closed polygon $\overline{\mathcal{P}}$ in a thin ribbon $\widetilde{R} \cap \overline{\mathcal{P}}$ that spans the space between $\partial\mathcal{P}$ and the lifted boundary $\widetilde{\partial R}$. This lifted ribbon gives us a mechanism for aligning $\partial\mathcal{P}$ and $\widetilde{\partial R}$.

In the right hand panel of Figure 1 the black node lying over z_j is labeled by v_j . The circuit also allows us to label the white nodes by w_j , so that in the counter-clockwise travel along $\partial\mathcal{P}$, w_j lies between v_{j-1} and v_j , indices mod t . Correspondingly, v_j lies between w_j and w_{j+1} , again indices mod t . Every edge e_j in \mathcal{E}_1 has two lifts in $\partial\mathcal{P}$, which we denote by e_j^+ and e_j^- . When travelling around the boundary of the lifted ribbon graph, e_j^+ corresponds to travelling outward along the spoke (z_0, z_j) and e_j^- corresponds to travelling inward along the spoke (z_j, z_0) . As previously described, in Figure 2 the portions corresponding to e_j^+ and e_j^- are indicated by + and - signs. We observe that

$$v_j = e_j^+ \cap e_j^- \text{ and } w_j = e_j^+ \cap e_{j-1}^-.$$

Our construction shows that every lifted polygon can be given a boundary structure and labelling that satisfies items 1-4 of Assumption 10. For item 5 of Assumption 10, we must now fix a distinguished polygon, which we still label \mathcal{P} . All other lifted polygons have the form $g\mathcal{P}$ for some $g \in G$. Having chosen \mathcal{P} , we must restrict the lifting homomorphism λ to be based at the unique point $\tilde{w} \in \mathcal{P}$ lying over the base point w . With this restriction, item 5 will hold.

Our lifted geometric objects v_j , w_j , e_j^+ , and e_j^- will now refer to the lifts of vertices and edges in $\widetilde{\mathcal{E}}_1$ lying in the boundary $\partial\mathcal{P}$ of the distinguished polygon. There is a *side pairing transformation* $\sigma_{e_j} \in G$ such that σ_{e_j} maps e_j^+ to e_j^- in an orientation reversing manner and

$$e_j^- = \mathcal{P} \cap \sigma_{e_j} \mathcal{P}.$$

Cellular homology in the single faced case. We now select our bases of $H_n(X^n, X^{n-1})$ in direct sum format. We first need to enumerate the cells. As noted, the open 2-cells are $g\mathcal{P}$, $g \in G$. The open 1-cells are ge_j^+ , $g \in G$, noting that $e_j^- = \sigma_{e_j} e_j^+$. In [7] it was determined that $\sigma_{e_j} = c_j^{-1}$ so that

$$(27) \quad e_j^- = c_j^{-1} e_j^+,$$

with orientation reversed. For 0-cells we use the quantities w_j and v_j to denote the lifts of vertices in \mathcal{E}_1 to the closure of \mathcal{P} . Consequently, we can say

$$(28) \quad e_j^+ = (w_j, v_j) \text{ and } e_j^- = (v_j, w_{j+1}),$$

indices modulo t . From equations (27) and (28) we see that $w_{j+1} = c_j^{-1}w_j$ and so

$$(29) \quad w_{j+1} = c_j^{-1} \cdots c_1^{-1}w_1 = h_j^{-1}w_1 \text{ for } 1 < j < t,$$

where $h_j = c_1 \cdots c_j$ ($h_0 = 1$). Thus, the 0-cells are $gw_1, g \in G$ and hw_j for $h \in G/\langle c_j \rangle$. So, in direct sum format, we may write

$$(30) \quad H_2(X^2/X^1) = \bigoplus_{g \in G} \mathbb{Z}g\mathcal{P},$$

$$(31) \quad H_1(X^1/X^0) = \bigoplus_{j=1}^t \bigoplus_{g \in G} \mathbb{Z}ge_j^+,$$

$$(32) \quad \tilde{H}_0(X^0) = \left(\bigoplus_{j=1}^t \bigoplus_{h \in G/\langle c_j \rangle} \mathbb{Z}hv_j \right) \bigoplus \left(\bigoplus_{g \in G} \mathbb{Z}w_1 \right).$$

Finally, we can write down the formulas for boundary maps

$$(33) \quad \partial_2(g\mathcal{P}) = g\partial_2(\mathcal{P}) = \sum_{j=1}^t ge_j^+ - gc_j^{-1}e_j^+,$$

and

$$(34) \quad \partial_1(ge_j^+) = g\partial_1(e_j^+) = gv_j - gw_j,$$

$$(35) \quad = gv_j - gh_{j-1}^{-1}w_1,$$

$$(36) \quad \partial_1(ge_j^-) = gc_j^{-1}\partial_1(e_j^+) = -gc_j^{-1}v_j + gc_j^{-1}h_{j-1}^{-1}w_1,$$

$$(37) \quad = gh_{j-1}^{-1}w_1 - gv_j.$$

4.3. The two faced case. We propose an alternative map (T, \mathcal{E}_2) for spherical T , it has the advantage of starting off as a CW -regular map.

As in the single faced case we may assume that the branch points are $t \geq 3$ equally spaced points on the equator of T with the same arrangement of branch points as in the single faced case. We choose a planar representation of T by stereographic projection to \mathbb{C} so that the south pole corresponds to the origin. Now we construct a cell complex on T as follows. There are two 2-cells: the upper and lower hemispheres. In the plane representation these 2-cells are the open unit disc and the interior of the complement of the unit disc, completed by the point at infinity. The points on the equator determine a series of t arcs, e_j , which are the 1-cells. We chain them together to form \mathcal{E}_2 . The t branch points z_j are the 0-cells. We think of T as two regular polygons with three or more sides glued together along corresponding edges. Over the open 2-cells and 1-cells π_G is unramified and hence in

S the lifts of 2-cells and the 1-cells are polygons and arcs upon which G acts freely. Note that the lifts of the closed two cells and the closed 1-cells map homeomorphically onto their images in T since their vertices are all distinct.

Now we determine a specific labelling of the cells in S . Let \mathcal{P}_L denote a specific polygon lying over the lower half sphere and $\tilde{e}_1, \dots, \tilde{e}_t$ the edges of \mathcal{P}_L with a counter-clockwise ordering induced from the lower hemisphere. For 0-cells we let v_1, \dots, v_t be the vertices of \mathcal{P}_L , with v_j lying over z_j . Consequently, \tilde{e}_j starts at v_{j-1} and ends at v_j (indices modulo t). The vertices and branch points also have a counter-clockwise ordering. There is a unique polygon \mathcal{P}_U lying over the upper hemisphere such that \mathcal{P}_L and \mathcal{P}_U meet along the edge \tilde{e}_1 . A counter-clockwise circuit around \mathcal{P}_U induces the opposite ordering on edges in T and vertices and reverses orientation induced on the edges.

The 2-cells of S have the form $g\mathcal{P}_L$ and $g\mathcal{P}_U$, $g \in G$, and there are $2|G|$ of them. We call the $g\mathcal{P}_L$ lower faces and the $g\mathcal{P}_U$ upper faces. The 1-cells have the form $g\tilde{e}_j$, $g \in G$ and there are $t|G|$ of them. We say that the edges of the form $g\tilde{e}_j$ have type j . The 0-cells or vertices have the form gv_j though they are not all distinct as we vary g . As in the case of edges, vertices of the form gv_j have type j .

Now we pick a specific base point $w = 0 \in \mathcal{P}_L$ and generating set of $\pi_1(T^\circ, w)$ to construct the generating vector from the monodromy map $\xi : \pi_1(T^\circ, w) \rightarrow G$. Let γ_j be the loop that starts at w , follows an imaginary spoke to the branch point corresponding to z_j , makes a small counter-clockwise loop around the branch point and heads back along the spoke to w . Our generating vector (c_1, \dots, c_t) is given by $c_j = \xi(\gamma_j)$. With these choices, the element c_j fixes v_j and permutes the faces with vertex corner v_i by a counterclockwise rotation through angle $2\pi/n_j$. The lower and upper faces are placed in an alternating fashion around v_i .

For homology computations it is important for us to know the labels of the t edges that form the boundary of \mathcal{P}_U . By simple transitivity, for each edge \tilde{e}_j of \mathcal{P}_L there is a unique $k_j \in G$ such that the lower face $k_j\mathcal{P}_L$ meets \mathcal{P}_U along $k_j\tilde{e}_j$. We may determine k_j by path lifting. Let γ be a loop in T° starting at w , crossing the edge e_1 transversally into the upper hemisphere, and then crossing back into the lower hemisphere through the edge e_j back to w . The path crosses edges only as specified and lies entirely in T° . Consider the lifted path $\tilde{\gamma}$ that starts at $\tilde{w} \in \mathcal{P}_L$, lying over w , crosses \tilde{e}_1 into \mathcal{P}_U , crosses $k_j\tilde{e}_j$ back into $k_j\mathcal{P}_L$ and ends up at $\tilde{\gamma}(1) = \xi(\gamma)\tilde{w} = k_j\tilde{w}$. It is not hard to show that $\gamma = \gamma_1 \cdots \gamma_{j-1}$

so that

$$k_j = \xi(\gamma) = \xi(\gamma_1) \cdots \xi(\gamma_{j-1}) = c_1 \cdots c_{j-1} = h_{j-1},$$

as previously defined.

Here are the boundary maps

$$(38) \quad \partial_2(g\mathcal{P}_L) = \sum_{j=1}^t g\tilde{e}_j,$$

$$(39) \quad \partial_2(g\mathcal{P}_U) = -\sum_{j=1}^t gk_j\tilde{e}_j,$$

$$(40) \quad \partial_1(g\tilde{e}_j) = gv_j - gv_{j-1}.$$

5. THE HOMOLOGY CALCULATION ALGORITHM

Our homology calculation and the G action $g \rightarrow \rho(g)$ upon it is now a linear algebra problem to be implemented as a computer calculation in Sage. By definition $H_1(S; \mathbb{Z}) = \ker(\partial_1)/\text{im}(\partial_2)$. The chain group $H_1(X^1/X^0)$ is a free \mathbb{Z} module of rank $t|G|$ with a \mathbb{Z} basis indexed by t copies of G . We must identify a basis for $\ker(\partial_1)$ and then a basis for a complementary subspace for $\text{im}(\partial_2)$. We propose to do this by Gaussian elimination on large matrices M_1, M_2 representing the operators ∂_1 and ∂_2 respectively.

To organize our vectors and matrices, we first make an ordered list of the elements of G : $g_1 = 1, g_2, \dots, g_{|G|}$. Then our ordering of components of vectors corresponding to 1-cells will be based an ordering of the pairs (g_i, e_j) lexicographic on the the pair (j, i) , where e_j is an edge in \mathcal{E} . The same remarks apply to 2-cells and 0-cells but some care is needed for the 0-cells as transversals of $G/\langle c_j \rangle$ will be required.

5.1. Some linear algebra. A key step of our process will be selecting a basis from a spanning set of a subspace. Here is a basic lemma concerning such a selection which is true for vector spaces over fields. It follows from a careful examination of Gaussian elimination as taught in a first course in linear algebra.

Lemma 11. *Let*

$$M = [C_1 \quad \cdots \quad C_n]$$

be a matrix written as a row of column vectors. Let M' be the matrix M after performing Gaussian elimination, using row operations. Let $P \subseteq \{1, \dots, n\}$ be the set of indices of the pivot columns of M' . Then, the set of vectors $\{C_i : i \in P\}$ is a basis of the column space of M .

Moreover, $m \in P$ if and only if C_m is not in the linear span of the columns that precede it.

Our next lemma will aid us in computing the G action, but first we set up the notation and a bit of background for the lemma. Let $V \subset W$ be two subspaces of an ambient vector space, and let

$$(41) \quad R = [C_1 \ \cdots \ C_m \ D_1 \ \cdots \ D_n] = [C \ D]$$

be a matrix with independent columns such that C_1, \dots, C_m is a basis of V and W is the column space of R . We can set up local coordinates on V and W/V by writing for $Y \in W$:

$$(42) \quad Y = CY_C + DY_D.$$

where Y_C, Y_D are unique column vectors of the length m and n respectively. It is not hard to show that the maps defined by

$$(43) \quad Y_C \rightarrow CY_C \text{ and } Y_D \rightarrow DY_D + V$$

are isomorphisms onto V and W/V , respectively.

Now, Let L be a matrix that induces a linear transformation $Y \rightarrow LY$ in the ambient space. Also denoting the transformation by L , we assume that $L(V) \subseteq V$ and $L(W) \subseteq W$, and hence L induces a linear transformation L_Q on W/V . Next we write

$$LCY_C = CY'_C \text{ and } LDY_D = CY''_C + DY'_D.$$

There is no D term in the first equation since V is L -invariant. The maps $Y_C \rightarrow Y'_C$ and $Y_D \rightarrow Y'_D$ are the induced maps on V and W/V , in local coordinates. The first statement is clear, for the second we note that at the coset level

$$L_Q(DY_D + V) = CY''_C + DY'_D + V = DY'_D + V.$$

We want to find matrices L_C, L_D of appropriate size such that

$$(44) \quad Y'_C = L_C Y_C \text{ and } Y'_D = L_D Y_D.$$

Inspired by the method of finding the normal equations for least squares, we need to find compatible left inverses for C and D . Indeed, as $R = [C \ D]$ has independent columns, it has a left inverse:

$$(45) \quad \begin{bmatrix} A \\ B \end{bmatrix} [C \ D] = \begin{bmatrix} AC & AD \\ BC & BD \end{bmatrix} = \begin{bmatrix} I_m & 0 \\ 0 & I_n \end{bmatrix},$$

for suitable matrices A, B . Then,

$$ALCY_C = ACY'_C = Y'_C$$

and

$$BLDY_D = BCY''_C + BDY'_D = Y'_D.$$

We select

$$(46) \quad L_C = ALC \text{ and } L_D = BLD$$

The preceding discussion proves the following lemma.

Lemma 12. *Let notation be as above. Then:*

- (1) *The images of $D_1 \dots, D_n$ in W/V form a basis for W/V .*
- (2) *There are local coordinate vectors Y_C and Y_D for V and W/V such that the maps in (43) are isomorphisms onto V and W/V .*
- (3) *Let L be a matrix inducing a linear transformation $L : Y \rightarrow LY$ on the ambient space, that satisfies $L(V) = V$ and $L(W) = W$. Let A, B be the components of a left inverse of R as defined in (45). Then in the local coordinates, Y_C and Y_D , the induced linear transformation of L on V and W/V are given by equations (44) and (46)*

5.2. Steps for computing homology representation. Here now are the steps for finding the homology representation.

- (1) Set up vector coordinates for the chain group $H_1(X^1/X^0)$ as suggested in the opening paragraphs of this section.
- (2) Calculate the matrices M_1 and M_2 of the differentials ∂_1 and ∂_2 , also as described in the opening paragraphs of this section.
- (3) Using the rows of M_2 , and Lemma 11, find a basis for $im(\partial_2)$. Fill in the C portion of the matrix R in (41) with this basis.
- (4) Find a basis for the null space of M_1 .
- (5) Make a temporary matrix $R' = [C \ D']$, where D' is filled in with the basis from the previous step.
- (6) Using Gaussian elimination on R' as described in Lemma 11, prune out the columns of D' that are dependent on the columns of C , resulting in $R = [C \ D]$.
- (7) Find a left inverse of R as in equation (45). The left inverse can be found using the standard method of finding right inverses using Gaussian elimination of an augmented matrix applied to R^T .
- (8) Select $g \in G$ for which a homology transformation matrix $\rho(g)$ is desired. Create the matrix

$$R^g = [C^g \ D^g]$$

by applying the transformation induced by g on $H_1(X^1/X^0)$ to all the columns of R . The matrix L of Lemma 12 need not be created, we need only create the modified columns in C^g and D^g .

- (9) Use Lemma 12 to find the desired matrix.

Remark 13. *According to Hatcher [14], cellular homology with coefficients works as described above with some attention paid to the cellular boundary formula (25). In that formula, β_j^{n-1} lies in the coefficient group and $d_{i,j}\beta_j^{n-1}$ is simply the \mathbb{Z} module action of multiplying a coefficient by an integer. The remainder of this section works without change when the coefficient group is a field, in particular \mathbb{Z}_2 coefficients.*

6. THE INTERSECTION FORM AND MATRIX

The intersection form $a \frown b$ on a surface S is a skew-symmetric R -bilinear form on $H_1(S; R)$, where R is any unital commutative ring. The form is invariant under the action of G on S . Once a basis $a_1, \dots, a_{2\sigma}$ of $H_1(S; R)$ is chosen we may construct the *intersection matrix*

$$I_S = [a_i \frown a_j].$$

Suppose $X = (x_1, \dots, x_{2\sigma})$ and $Y = (y_1, \dots, y_{2\sigma})$ are two R -vectors and $a_X = x_1 a_1 + \dots + x_{2\sigma} a_{2\sigma}$ and $a_Y = y_1 a_1 + \dots + y_{2\sigma} a_{2\sigma}$ are the corresponding homology classes. Then

$$a_X \frown a_Y = X^\top I_S Y.$$

Through a change of basis the intersection matrix may be brought to canonical form $\begin{pmatrix} 0 & I \\ -I & 0 \end{pmatrix}$, whereby the matrices of the homology representation become symplectic, taking values in $Sp_{2\sigma}(R)$. As this shall be necessary for the application to theta characteristics in §7.4, we shall briefly describe how this may be implemented, restricting to the two faced case of §4.3.

It may be shown that if a^\top and b^\top are the Poincaré duals of a, b , respectively then

$$a \frown b = (a^\top \smile b^\top) \frown [S],$$

where \smile denotes the cup product in cohomology and $[S]$ is the fundamental homology 2-class of S . An explicit formula for the cup product in simplicial cohomology is given in [14, §3.2], and we may use this in our implementation provided we refine the CW -complex on S to a simplicial complex. In the case $t = 3$ there is no change to the complex. In the $t > 3$ case this refinement may be achieved by adding additional edges through the upper and lower faces, see Appendix A. This does increase the dimension of the matrices which must be used in the computation of the homology basis. Refining the complex by adding additional edges (and so also additional faces) has the effect of modifying the differentials $\partial_{1,2}$ from those defined earlier, but the

remaining method for computing the homology basis and the action of G on it carries through.

By using the cup product formula we avoid the problem present in other works of having to find representatives of homology classes, and avoid difficulties in correctly signing intersections. As computational implementation of the cup product in simplicial cohomology is well known, for example see [9], we shall not discuss the details further here.

7. EXAMPLES AND COMPUTATION

7.1. Hyperelliptic example. As a demonstration of how the procedure works, we shall apply the algorithm to S determined by $G = \langle \iota \mid \iota^2 = 1 \rangle$ acting with signature $(0; 2, 2, 2, 2)$ and generating vector $(\iota, \iota, \iota, \iota)$. This is the action of the hyperelliptic involution on a genus-1 surface.

Remark 14. *Note this surface S is not hyperbolic, but the group action considered is still faithful and the method still applies.*

M_2 is the $t|G| \times 2|G|$ matrix (in the case of the hyperelliptic involution $|G| = 2$ and $t = 2\sigma + 2$) which acts on column vectors representing 2-cells ordered as

$$g_1\mathcal{P}_L, \dots, g_{|G|}\mathcal{P}_L, g_1\mathcal{P}_U, \dots, g_{|G|}\mathcal{P}_U,$$

by left multiplication. The output column vectors correspond to 1-cells ordered as

$$g_1\tilde{e}_1, \dots, g_{|G|}\tilde{e}_1, g_1\tilde{e}_2, \dots, g_{|G|}\tilde{e}_t.$$

As such, introducing the $|G| \times |G|$ matrices $\rho_i = \rho_R(k_i)$ the images of k_i under the right-multiplication representation of G on itself, we find

$$M_2 = \begin{pmatrix} I_{|G|} & -\rho_1 \\ \vdots & \vdots \\ I_{|G|} & -\rho_t \end{pmatrix},$$

where I_n is the $n \times n$ identity matrix.

Likewise, if we introduce the $\frac{|G|}{n_i} \times |G|$ matrices P_i which act by left multiplication on column vectors of length $|G|$ to project elements $g \in G$ to their left coset $g\langle c_i \rangle$, then we have M_1 is the matrix

$$M_1 = \begin{pmatrix} P_1 & -P_1 & 0 & \dots & 0 \\ 0 & P_2 & -P_2 & \dots & 0 \\ \vdots & \vdots & \ddots & \ddots & 0 \\ 0 & \vdots & 0 & P_{t-1} & -P_{t-1} \\ -P_t & 0 & \dots & 0 & P_t \end{pmatrix}.$$

In the case at hand we see

$$\rho_i = \begin{cases} I_2, & i \text{ odd,} \\ \begin{pmatrix} 0 & 1 \\ 1 & 0 \end{pmatrix}, & i \text{ even,} \end{cases} \quad \text{and} \quad P_i = (1 \ \dots \ 1).$$

Following the procedure laid out one ends up finding that

$$D = \begin{pmatrix} 1 & 0 \\ 0 & 0 \\ 0 & 1 \\ 1 & -1 \\ 0 & 0 \\ 1 & 0 \\ 0 & 0 \\ 1 & 0 \end{pmatrix}, \quad B = \begin{pmatrix} 1 & 0 & 0 & 0 & -1 & 0 & 0 & 0 \\ 0 & 0 & 1 & 0 & 0 & 0 & -1 & 0 \end{pmatrix}.$$

Moreover matrix L corresponding to the action of g is

$$L = \bigoplus_{i=1}^t \rho_L(g),$$

where ρ_L is the left-multiplication representation of G on itself. As such $\rho_L(\iota) = \begin{pmatrix} 0 & 1 \\ 1 & 0 \end{pmatrix}$, and one may verify $L_D = -I_2$ as is to be expected for the homology action of the hyperelliptic involution.

7.2. Implementation comments. The algorithm is implemented in Sage using the complex of the two faced case, and so being valid when $\tau = 0$. It is available from https://github.com/DisneyHogg/homology_representation/.

Some comments about the implementation are appropriate.

- GAP is used to get the permutation representation of G acting on the cosets $G/\langle c_i \rangle$.
- The matrices M_1, M_2 are implemented as sparse matrices in an endeavor to keep the algorithm as memory efficient as possible when $|G|$ gets large. This proves to be a sensible choice; our implementation is able to compute the representation of $\text{Aut}(S)$ on $H_1(S; \mathbb{Z}_2)$ for the modular curves $S = X(13), X(17)$, which existing algorithms are unable to due to memory issues (see §7.4).
- It is convenient when computing the intersection form to work directly with cohomology rather than homology, but the material effect of this is just to work with row vectors from the beginning rather than column vectors and later transposing.

7.3. Performance comparison. In order to evaluate the performance of our new algorithm, we wish to compare to existing methodologies (especially memory efficiency), namely that from [2]. For both algorithms we found the time taken to compute the representation on $H_1(S; \mathbb{Z})$ of the G action for all 1897 topologically inequivalent generating vectors acting in genera $2 \leq \sigma \leq 12$, the latter data generated using [1]. These runtimes will naturally be hardware dependent; computations were run on an Intel Core i5-8350U CPU at 1.70GHz. At this level we see that our new algorithm is on average $1.2 \times$ faster.

Moreover, one key motivation of this paper was to have a methodology which performed better when computing the representation on $H_1(S; \mathbb{Z}_2)$, as this is required for computing orbits of theta characteristics (see the later discussion in §7.4). As such we recomputed the runtime in this scenario and again compare the performance, seeing now that the computation is on average $2 \times$ faster.

Somewhat more importantly, as the genus of the curve increases our new method appears to have better memory efficiency, rendering new ranges of genera amenable to computation. We ran both algorithms to compute the homology representation of C_p acting with signature $(0; p, p, p)$ for increasing p an odd prime, which acts on a surface of genus $\sigma = \frac{p-1}{2}$. The method of [2] was unable to compute the representation for $p \geq 79$ due to overflow errors, but our new algorithm continued to work and answer in less than one second up to $p = 331$.

7.4. Theta characteristics. As previously mentioned, an important application for us of this method will be computing the action of G on $H_1(S; \mathbb{Z}_2)$, because of its role in computing the orbits of theta characteristics [15, 4]; these are line bundles $L \rightarrow S$ such that $L^{\otimes 2} \cong K_S$ which may be identified with elements of $H_1(S; \mathbb{Z}_2)$, such that the induced action of $\text{Aut}(S)$ on theta characteristics becomes an affine action of the homology representation on $H_1(S; \mathbb{Z}_2)$.

In particular we consider the modular curves $X(p)$, $p \geq 7$ an odd prime. These are curves of genus $\sigma = \frac{1}{24}(p+2)(p-3)(p-5)$ that have an action of $PSL(2, p)$ with signature $(0; 2, 3, p)$. The results developed in [4] yield that these curves should have a unique invariant characteristic, and we seek to verify that numerically where possible. While the code of [2] works in the cases $p = 7, 11$, it does not complete for larger p . Using our new method we can check $p = 13, 17$, verifying the theoretical results.

Moreover, with the homology representation in hand we can compute the parity of the invariant characteristic, which at present is unable to be determined by theory alone in most cases. We find that the unique

invariant characteristic always has even parity for $p = 7, 11, 13, 17$: we conjectured that this was always the case, a result which has subsequently been proven [8].

APPENDIX A. DETAILS OF 2-FACE SIMPLICIAL COMPLEX

Here we give further details of how the CW -complex constructed in the 2-face case with $t > 3$ is refined to give a simplicial complex in order to use the cup product to compute the intersection form.

From the map (T, \mathcal{E}_2) we construct a map (T, \mathcal{E}'_2) by adding arcs from z_1 to z_i ($i = 3, \dots, t-1$) in each hemisphere, denoted l_i, u_i . Lifting this as before the 1-cells on S are $g\tilde{e}_j$ ($j = 1, \dots, t$) and $g\tilde{l}_i, g\tilde{u}_i$ ($i = 3, \dots, t-1$). The new 1-cells have differentials

$$\partial_1(g\tilde{l}_i) = gv_i - gv_1, \quad \partial_1(g\tilde{u}_i) = gk_i v_i - gk_1 v_1.$$

The 2-cells on S are now gL_i, gU_i , ($i = 3, \dots, t$) which are lifts of faces on the lower and upper hemisphere respectively with differentials

$$\partial_2(gL_i) = g\tilde{e}_i - g\tilde{l}_i + g\tilde{l}_{i-1}, \quad \partial_2(gU_i) = gk_i \tilde{e}_i - g\tilde{u}_i + g\tilde{u}_{i-1},$$

where we have defined $g\tilde{l}_2 := g\tilde{e}_2$, $g\tilde{l}_t := -g\tilde{e}_1$, $g\tilde{u}_2 = gk_2 \tilde{e}_2$, $g\tilde{u}_t = -gk_1 \tilde{e}_1$. We have the interpretation in our mind that

$$g\mathcal{P}_L = \sum_{i=3}^t gL_i, \quad g\mathcal{P}_U = - \sum_{i=3}^t gU_i.$$

REFERENCES

- [1] A. Behn, A. M. , Rojas, and M. Tello-Carrera. A SAGE package for n-gonal equisymmetric stratification of \mathcal{M}_g . *Experimental Mathematics*, 32(1):54–69, Jan. 2023.
- [2] A. Behn, R. E. Rodríguez, and A. M. Rojas. Adapted hyperbolic polygons and symplectic representations for group actions on Riemann surfaces. *Journal of Pure and Applied Algebra*, 217(3):409–426, 2013.
- [3] W. Bosma, J. Cannon, and C. Playoust. The Magma algebra system. I. The user language. *J. Symbolic Comput.*, 24(3-4):235–265, 1997. Computational algebra and number theory (London, 1993).
- [4] H. W. Braden and L. Disney-Hogg. Orbits of theta characteristics. *Experimental Mathematics*, pages 1–50, 2025.
- [5] S. A. Broughton. The equisymmetric stratification of the moduli space and the Krull dimension of mapping class groups. *Topology and its Applications*, 37(2):101–113, 1990.
- [6] S. A. Broughton. Equivalence of finite group actions on Riemann surfaces and algebraic curves. In *Automorphisms of Riemann surfaces, subgroups of mapping class groups and related topics*, volume 776 of *Contemporary Mathematics*, page 353. American Mathematical Society, 2022.

- [7] S. A. Broughton, A. F. Costa, and M. Izquierdo. Modular companions in planar one-dimensional equisymmetric strata. In *Algebraic and Topological Interplay of Algebraic Varieties: A Conference in Honor of E. Artal's 60th and A. Melle's 55th Birthdays*, Contemporary Mathematics, pages 109–145, 2026.
- [8] L. Disney-Hogg. The parity of invariant characteristics. Unpublished results.
- [9] The GAP Group. *GAP – Groups, Algorithms, and Programming, Version 4.12.2*, 2022.
- [10] J. Gilman. Canonical symplectic representations for prime order conjugacy classes of the mapping-class group. *Journal of Algebra*, 318(1):430–455, 2007.
- [11] J. Gilman. Prime order automorphism of Riemann surfaces. In *Teichmüller theory and moduli problem. Proceedings of the workshop at Harish-Chandra Research Institute, Allahabad, India, January 5–15, 2006*, pages 229–246. Mysore: Ramanujan Mathematical Society, 2010.
- [12] J. Gilman. Computing adapted bases for conformal automorphism groups of Riemann surfaces. In *Riemann and Klein surfaces, automorphisms, symmetries and moduli spaces. Conference in honour of Emilio Bujalance, Linköping, Sweden, June 24–28, 2013*, pages 137–153. Providence, RI: American Mathematical Society (AMS), 2015.
- [13] J. Gilman and D. Patterson. Intersection matrices for bases adapted to automorphisms of a compact Riemann surface. In *Riemann surfaces and related topics. Proceedings of the 1978 Stony Brook Conference. (AM-97)*, Annals of Mathematics Studies, pages 149–166. Princeton University Press, 1981.
- [14] A. Hatcher. *Algebraic topology*. Cambridge University Press, 2002.
- [15] S. Kallel and D. Sjerve. Invariant spin structures on Riemann surfaces. *Annales de la Faculté des Sciences de Toulouse*, 19:457–477, 2010.
- [16] The Sage Developers. SageMath, the Sage Mathematics Software System (Version 9.7). <https://www.sagemath.org>, 2022.